Changes in glacier dynamics at the northern Antarctic Peninsula since 1985

Thorsten Seehaus[1], Alison Cook[2], Aline B. Silva[3], Matthias Braun[1]

[1] Institute of Geography, Friedrich-Alexander-University Erlangen-Nuremberg, Wetterkreuz 15, 91058 Erlangen, Germany

5 [2] Department of Geography, Durham University, South Road, Durham DH1 3LE, United Kingdom

[3] Laboratório de Monitoramento da Criosfera, Universidade Federal do Rio Grande, Av. Itália, km 8, 96203-900, Rio Grande - RS Brazil

Correspondence to: Thorsten Seehaus (*thorsten.seehaus@fau.de*)

Abstract. The climatic conditions along the northern Antarctic Peninsula have shown significant changes within the last 50

10 years. Most studies have focused on the glaciers affected by the disintegration of the ice shelves along the east coast. However, temporally and spatially detailed observations of the changes in ice dynamics along both the east and west coastlines are missing. Temporal trends of glacier area (1985-2015) and ice surface velocity (1992-2014) changes are derived from a broad multi-mission remote sensing database for 74 glacier basins on the northern Antarctic Peninsula (<65° S). A recession of the glaciers by 238.81 km² is found for the period 1985-2015, whereas the glaciers affected by ice shelf

15 disintegration showed the largest retreat by 208.59 km². Glaciers on the east coast north of the former Prince Gustav Ice Shelf receded by only 21.07 km² and decelerated by about 69 % on average. Whereat, the former ice shelf tributary glaciers on the east coast showed similar temporal ice dynamics trends. A dramatic acceleration after ice shelf disintegration with a subsequent deceleration is observed. In 2014, the flow speed of the former ice shelf tributaries was 16.8 % higher than at the beginning of the study period. Along the west coast the average flow speeds of the glaciers increased by 41.5 %. However,

20 the glaciers on the western Antarctic Peninsula revealed a strong spatial variability of the changes in ice dynamics. By applying a hierarchical cluster analysis we show that this is associated with geometric parameters of the individual glacier basin. The heterogeneous pattern of ice dynamic trends at the northern Antarctic Peninsula points out that temporally and spatially detailed observations as well as further monitoring are necessary to reveal the full picture of glacier change in regions with such strong topographic and climatic gradients.

1 Introduction

During the last century, the Antarctic Peninsula (AP) has undergone significant warming (Carcass et al., 1998; Turner et al., 2005), leading to substantial glaciological changes. Shepherd et al. (2012) compiled a comprehensive glacier mass balance database of the polar ice sheets. The authors reported a mass loss on the whole AP (<73° S) of -36±10 Gt a-1 for the period 2005-2010, which corresponds to 35% of the total mass loss of Antarctica. A projection of sea level rise contribution by the

30 AP ice sheet amounts to 7-16 mm sea-level equivalent by 2100 and 10-25 mm by 2200 (Barrand et al., 2013a). However,

along the western AP and on the higher elevation regions an increase in snow accumulation in the late 20th century was derived from ice cores (e.g. at Bruce Plateau, 66.03°S, 64.07°W, Goodwind, 2013; at Detroit Plateau, 64.08°S, 59.68° W, Potocki et al., 2011, Palmer Land, 73.59° S, 70.36° W, Thomas et al., 2008) and climate models (e.g. Dee et al., 2011), whereas van Wessem et al. (2016) obtained insignificant trends in precipitation.

5 Numerous ice shelves along the AP (e.g. Larsen A/B, Prince Gustav and Wordie) have retreated widely or disintegrated in recent decades (Cook and Vaughan, 2010). As a consequence to the reduced buttressing, former tributary glaciers showed increased ice discharge and frontal retreat (e.g. De Angelis and Skvarca, 2003; Rack and Rott, 2004; Rignot et al., 2004; Seehaus et al., 2015; Wendt et al., 2010). For the northern AP (<66° S), a mass loss rate of -24.9±7.8 Gt a-1 was reported by Scambos et al. (2014) for the period 2003-2008, indicating that major ice mass depletion happened at the northern part of the
10 peninsula, especially along the eastern side where numerous glaciers have been affected by ice shelf collapses. Seehaus et al. (2015, 2016) quantified the ice loss of former ice shelf tributaries. Mass loss rates of -2.14±0.21 Gt a^{-1} (1995-2014) and -1.16±0.16 Gt a^{-1} (1993-2014) were found at Dinsmoor-Bombardier-Edgeworth Glacier System and Sjögren-Inlet glaciers, respectively. Glaciers that were not terminating in an ice shelf also showed considerable changes. Cook et al. (2005, 2014) have analyzed the variations of tidewater glacier fronts since the 1940s. The authors reported that 90% of the observed
15 glaciers retreated, which they partly attributed to atmospheric warming. A more recent study revealed a mid-ocean warming along the southwestern coast of the AP, forcing the glacier retreat in this region (Cook et al., 2016). Pritchard and Vaughan (2007) observed an acceleration of ice flow by ~12% along the west coast of the AP (1995-2005) and linked it to frontal retreat and dynamic thinning of the tidewater glaciers. Observations by Kunz et al. (2012) support this supposition. The authors analyzed surface elevation changes at 12 glaciers on the western AP based on stereoscopic digital elevation models
20 (DEM) over the period 1947-2010. Frontal surface lowering was found at all glaciers, whereas, area-wide surface lowering was observed on the north-eastern AP by various author groups (e.g. Berthier et al., 2012; Rott et al., 2014; Scambos et al., 2004; Wuite et al., 2015) as a consequence to ice shelf disintegration.

The observations suggest that the ice masses on the AP are contributing to sea level rise and show that glaciers' response to climate change on the AP is not homogeneous and that more detailed knowledge of various aspects on the glacier changes
25 are required. Previous studies often just cover a specific period or region, or focus on one particular aspect of glacier change. Therefore, we study the changes in glacier extent in combination with detailed investigations on ice dynamics as well as other derived geometrical attributes of glaciers on the northern AP (<65° S) between 1985 and 2015. We analyze various multi-mission remote sensing datasets in order to obtain methodically consistent and temporally detailed time series of ice dynamic trends of 74 glacier basins. The observations are individually discussed for the sub regions, considering the
30 different atmospheric, glaciological and oceanic conditions and changes.

2 Study site

The AP is the northern-most region of Antarctica. It covers only 3% of the entire continent, but receives 13% of the total mass input (van Lipzig et al., 2002, 2004). The AP acts as an orographic barrier for the circumpolar westerly air streams leading to very high precipitation values on the west coast and on the plateau region, as well as frequent foehn type wind occurrences on the east coast (Cape et al., 2015, Marshall et al., 2006). The foehn events are characterized by strong winds and high air temperatures. Consequently, the climatic mass balance (b_{clim}) shows a strong gradient across the mountain chain (Turner, 2002; van Wessem et al., 2016). Apart from those that are ice shelf tributaries, nearly all glaciers on the AP are marine terminating, and most of the glacier catchments extend up to the high elevation plateau regions. Usually the AP plateau is separated from the outlet glaciers by escarpments and ice-falls. Glaciers on the west coast drain into the Bellingshausen Sea and on the east coast into the Weddell Sea. Since the 1980s, the ice shelves along the east coast have substantially recessed and disintegrated (Prince Gustav and Larsen-A in 1995, Larsen Inlet in 1987-89 and Larsen-B in 2002) (Cook and Vaughan, 2010; Skvarca et al., 1999). Scambos et al. (2003) attributed the retreat and collapse of ice shelves to higher summer air temperatures and surface melt. The northern AP has a maritime climate and is the only region of Antarctica that experiences widespread surface melt (Barrand et al., 2013b; Rau and Braun, 2002).

Our study site stretches about 330 km from the northern tip of the AP southwards to Drygalski Glacier on the east coast and Grubb Glacier on the west coast (Fig. 1). This narrow mountain chain covers an area of ~11,000 km² with altitudes stretching from sea level up to 2220 m. The glacier basin delineations are based on the Antarctic Digital Database ADD 6.0 (Cook et al., 2014). Glacier names are taken from the Global Land Ice Measurements from Space (GLIMS) project database. The local GLIMS glacier IDs (e.g. TPE62, LAB2) are used for unnamed glaciers and further missing glacier basin names are substituted with the ADD 6.0 glacier IDs. Some basins with lateral connected termini are merged and in these cases, the names of the glaciers are also merged (e.g. Sikorsky-Breguet-Gregory – SBG, see Table 1 for abbreviations of glacier names). Due to the sparse data coverage, no time series analysis of the glaciers at the northern tip of the AP is possible. Therefore the northern-most analyzed catchments are Broad-Valley Glacier on the east coast and TPE8 Glacier on the west coast, resulting in 74 studied glacier basins. Furthermore, the study region is divided into three sectors, taking into account the different climatic settings, drainage orientation and former ice shelf extent: sector "West" - Glaciers on the west coast, draining into the Bransfield and Gerlache Strait, sector "East" – Glaciers on the east coast, draining into the Prince Gustav Channel; sector "East-Ice-Shelf" – Glaciers on the east coast, that were former tributaries to the Larsen-A, Larsen-Inlet and Prince Gustav Ice Shelf.

3 Data & Methods

3.1 Area changes

Changes in glacier area are derived by differencing glacier outlines from various epochs. All observed glaciers are tidewater glaciers and only area changes along the calving front were considered.

Information on the position of the glacier fronts at the study region are taken from Cook et al. (2014), and are available for the whole AP in the ADD 6.0 (1945-2010). This coastal-change inventory is based on manually digitized ice front positions using imagery from various satellite sensors (e.g. Landsat, ERS) and aerial photo campaigns. This dataset is updated (up to 2015) and gaps are filled by manual mapping of the ice front positions based on SAR, Landsat and ASTER images. According to Cook et al. (2014) the ice-front positions are assigned to 5-year intervals in order to analyze temporal trends in glacier area changes in the period 1985-2015. Before 1985, only sparse information on ice front positions for the whole study region is available, and the coverage by SAR data for analyzing glacier flow starts in 1992. The analysis of the area changes for the Larsen-A and Prince Gustav Ice Shelf tributaries is limited to the period 1995-2015, since the ice shelves disintegrated in 1995.

The uncertainties of the glacier change measurements strongly depend on the imagery used (e.g. spatial resolution, geodetic accuracies) as well as the methods used. To each record in the coastal-change inventory from the ADD 6.0, a reliability rating is assigned according to Ferrigno et al. (2006). The rating ranges from 1 to 5 (reliability within 60 m to 1 km) and takes into account errors due to manual digitization and interpretation (see Ferrigno et al., 2006 for a detailed description). This approach is also applied on the updated ice-front positions. Nearly all mapped ice fronts in the study region have a good reliability rating of 1 (76%) and 2 (21%). Only a few glacier fronts (3%) have a rating of 3. Reliability ratings of 4 and 5 are not applied.

3.2 Surface velocities

Surface velocity maps are derived from repeat-pass Synthetic Aperture Radar (SAR) acquisitions. SAR image time series of the satellite missions ERS-1/2, Envisat, RadarSAT-1, ALOS, TerraSAR-X (TSX) and TanDEM-X (TDX) are analyzed, covering the period 1992-2014. Specifications of the SAR sensors are listed in Table 2. The large number of SAR images was provided by the German Aerospace Center (DLR), the European Space Agency (ESA) and the Alaska Satellite Facility (ASF). To obtain displacement fields for the glaciers, the widely used and well approved intensity offset tracking method is applied on co-registered single look complex SAR image pairs (Strozzi et al., 2002). In order to improve the co-registration of the image pairs, we mask out fast moving and unstable regions such as outlet glaciers and the sea. Furthermore, single SAR image tiles acquired during the same satellite flyover are concatenated in the along-track direction. This helps to further improve the coregistration but also simplifies the analysis of the final results as no mosaicking of the results is needed.

Image pairs with low quality coregistration are filtered out. A moving window technique is used by the intensity offset tracking method to compute the cross-correlation function of each image patch and to derive its azimuth and slant range displacement. Less reliable offset measurements are filtered out by means of the signal-to-noise ratio of the normalized cross-correlation function. Moreover, we apply an additional filter algorithm based on a comparison of the magnitude and alignment of the displacement vector relative to its surrounding offset measurements. This technique removes more than 90% of incorrect measurements (Burgess et al., 2012). Finally, the displacement fields are transferred from slant range into ground range geometry, taking into account the effects on the local incidence angle by the topography, geocoded, orthorectified and converted into velocity fields by means of the time span between the SAR acquisitions. The ASTER Global Digital Elevation Model of the Antarctic Peninsula (AP-DEM, Cook et al., 2012) is used as elevation reference. The mean date of the consecutive SAR acquisitions is assigned to each velocity field.

Depending on the displacement rate, the tracking window size needs to be adapted. For the fast flowing central glacier sections, larger window sizes are needed since large displacements cannot be tracked by using small correlation patches. Small tracking window sizes are suitable for the slow moving lateral sections of the outlet glaciers. Wide parts of large tracking patches cover the stable area next to the glacier, which biases the tracking results towards lower velocities. Consequently, we compute surface velocity fields of the same image pairs for different correlation patch sizes in order to get the best spatial coverage. Table 2 shows the different tracking window sizes for each sensor. The results of each image pair are stacked by starting with the results of smallest tracking window size and filling the gaps with the results of the next biggest tracking window size.

The accuracy of the velocity measurements strongly depends on the coregistration quality and the intensity offset tracking algorithm settings. The mismatch of the coregistration σ_v^C is quantified by measuring the displacement on stable reference areas, like rock outcrops and nunataks. Based on the Bedmap2 (Fretwell et al., 2013) and ADD 6.0 rock outcrop masks, reference areas are defined and the median displacements magnitude of each velocity field is measured at these areas. The uncertainty of the tracking process σ_v^T is estimated according to McNabb et al. (2012) and Seehaus et al. (2015) depending on accuracy of the tracking algorithm C, image resolution Δx, oversampling factor z, time interval Δt.

$$\sigma_v^T = \frac{C\,\Delta x}{z\,\Delta t} \tag{1}$$

The accuracy of the tracking algorithm is estimated to be 0.2 pixels. Both independent error estimates are quadratically summed to compute the uncertainties of the individual velocity fields σ_v.

$$\sigma_v = \sqrt{(\sigma_v^T)^2 + (\sigma_v^C)^2} \tag{2}$$

Profiles are defined (red lines in Fig. 1) close to the terminus of each glacier basin, taking into account the temporal changes of ice front position. The magnitude and direction (relative to north direction) of ice flow along the profiles of each tracking result are visually inspected in order to check the quality. Datasets with partial profile coverage or large data gaps, as well as those with still remaining tracking errors, are rejected. The changes in the ice flow of each glacier are analyzed by measuring

5 the surface velocities within a buffer zone of 200m along the profiles, in order to reduce the number of data gap along the profile due to data voids in the velocity fields. To minimize the impact of potential outliers, median velocities along the profiles are calculated and the temporal trends are plotted. The glaciers are classified in six categories according to the temporal evolution of the ice flow speeds (see Table 3). Only glaciers with more than two observations and an observation period of more than 10 years are categorized. The GAMMA Remote Sensing software is used for processing of the SAR

10 data.

3.3 Catchment geometries and settings

Glacier velocities and area change measurements provide information on the ice dynamics of the individual glaciers. To facilitate a better and comprehensive interpretation of these observations, additional attributes regarding the different geometries and settings of the glaciers are derived.

15 Mass input strongly affects the dynamics of a glacier. The climatic mass balance at the northern AP shows a strong spatial variability, with very high accumulation rates along the west coast, significantly lower values on the east coast and an increase towards higher altitudes (Turner, 2002; van Wessem et al. 2016). Consequently, the mass input depends on the elevation range and the hypsometry. For each glacier basin a Hypsometric Index (HI), defined by Jiskoot et al. (2009), is calculated by means of surface elevations from the AP-DEM. Based on this index the glaciers are grouped into five

20 categories ranging from very top-heavy to very bottom heavy (Table 4). Moreover, the maximum elevations of the individual glacier catchments are derived from the AP-DEM, which represents the altitude range of the catchment, since all observed glaciers are marine terminating.

In order to characterize the catchment shape, the ratios (FA) of the flux gate cross sections divided by the glacier catchment areas are calculated. Lower values indicate a channelized outflow. Ice thickness at the flux gates is taken from the AP

25 Bedmap dataset from Huss and Farinotti (2014).

3.4 Cluster analysis

The glaciers in the sector "West" (Fig. 1, red shaded area) show a heterogeneous pattern of ice dynamics as compared to the other sectors changes (Section 4.1, 4.2). In order to analyze the influence of the glacier geometries on the glaciological changes and to find similarities, a cluster analysis is carried out in sector "West". Variables of the glacier dynamics used are

30 the derived area changes (in percent) and velocity changes (ratings of the categories, Table 3). The glacier geometry

parameters used are the Hypsometric Indexes HI, maximum surface elevation h_{max} of the basin and the flux gate to catchment size ratio FA. The variables are standardized by subtracting the variables mean value and dividing by it's mean absolute deviation. Afterwards a dissimilarity matrix is calculated using the Euclidean distances between the observations (Deza and Deza, 2009). A hierarchical cluster analysis (Kaufman and Rousseeuw, 1990) is applied on the dissimilarities using Ward's minimum variance method (Ward, 1963). At the start, for each glacier a cluster is defined and then the most similar clusters are iteratively joint until only one cluster is left. The distances between the clusters are updated in each iteration step by applying the Lance-Wiliams algorithms (Lance and Williams, 1967).

4 Results

4.1 Area changes

Area changes relative to the measurements in the epoch 1985-1989 of selected glaciers are plotted in Fig. 2 and of all observed glaciers in Fig. S1-S74 (supplement). The glaciers are classified in three groups based on the latest area change measurement: retreat (Fig. 2a, b, c, f) – loss of glacier area by frontal retreat; stable (Fig. 2e) – no significant area changes (within the error bars); advance (Fig. 2d) – gain of glacier area by frontal advance. In Fig. 3 the spatial distribution of the area change classification is illustrated. All glaciers along the east coast, including the former ice shelf tributaries, retreated, whereas along the west coast, numerous glaciers show stable ice front positions and some glaciers even advanced. In total, 238 km² of glacier area was lost at the study site in the period 1985-2015, which corresponds to a relative loss of 2.2%. All sectors show glacier area loss (Table 5), of which the area loss at sector "East-Ice-Shelves" clearly dominates. The temporal trends of total glacier area and area loss of all observed glaciers and of each sector are presented in Fig. 4. Catchment areas and changes between 1985 and 2015 of the individual basins are listed in Table S1 (supplement) and relative changes are illustrated in Fig. 5.

4.2 Surface velocities

In total 282 stacked and filtered velocity fields are derived from the SAR acquisitions covering the period from 25th December, 1992 until 16th December, 2014. The average total uncertainty of the velocity fields amounts to 0.08 m d^{-1}. In Table S2 (supplement) the error estimates of each velocity field are listed. The mean sample count to estimate the coregistration quality is 11717 and the average mismatch amounts to 0.07 m d^{-1}. The error caused by the tracking algorithm strongly varies depending on the source of the SAR data (sensor). A mean value of 0.05 m d^{-1} is found. ERS image pairs with time intervals of one day have very large tracking uncertainties, due to the very short temporal baselines, and are not considered in the total error computations.

All measured velocity profiles of the 74 observed glaciers are visually inspected and finally 2503 datasets passed the quality check (on average ~34 per glacier). Figure 2 shows by example the temporal evolution of the ice flow for each velocity change category (see Table 3). The temporal trends of the surface velocities at the termini of each glacier are plotted in Fig. S1-S74 (supplement) and the related categories are listed in Table S1 (supplement). The spatial distribution of the categories is illustrated in Fig. 3. At nearly all glaciers in sector "East-Ice-Shelf" a peak in ice velocities is observed. In the sector "East", most glaciers showed a decrease in flow velocities in the observation period. The glaciers on the west coast show a more irregular distribution than along the east coast, but some local clustering can be observed.

For each glacier the flow velocities in the first v_S and last year v_E of the observation period as well as the absolute and relative change dv is presented in Table S2 (supplement). The mean values of v_S, v_S and dv of all analyzed glaciers and for each sector are listed in Table 5. On average the ice flow in the study region increased by 1.6%. Along the west coast an average acceleration by 41.5% occurred and the former ice shelf tributaries on the east coast accelerated by 16.8%. In the sector "East" the glaciers decelerated resulting in a mean velocity change of -69%. The shortest observation period is 14.8 years at DBC31 Glacier and on average velocity changes are analyzed over a period of 19.4 years.

4.3 Catchment geometries and settings

The spatial distribution of Hypsometric Indexes and categories of the glacier basins is presented in Fig. 3 and the values are listed in Table S2 (supplement). No clear distribution pattern can be identified, reflecting the heterogeneous topography of the AP. The maximum elevation of the catchments and the FA factors are also listed in Table S2 (supplement).

4.4 Cluster analysis

The resulting dendrogram of the hierarchical cluster analysis is plotted in Fig. 6. Four groups are distinguished. The boxplots of each input variable are generated based on this grouping and are shown in Fig. 7. The characteristics of the groups are discussed in Section 5.3.

5 Discussion

Most of the observed glaciers (62%) retreated and only 8% advanced in the study period. These findings are comparable to the results of Cook et al. (2005, 2014, 2016). Only glaciers along the west coast showed stable or advancing calving fronts and all glaciers on the east coast receded. This heterogeneous pattern was also observed by Davies et al. (2012) on western Trinity Peninsula. Most significant retreat occurred in the sector "East-Ice-Shelf". In the period 1985-1995, the Larsen-Inlet tributaries (APPE-glaciers) lost 45.0 km² of ice. After the disintegration of Prince-Gustav and Larsen-A Ice Shelf, the tributaries rapidly retreated in the period 1995-2005. The recession slowed down in the latest observation interval (2005-2010). This trend is comparable to detailed observations by Seehaus et al. (2015, 2016) at individual glaciers (DBE glaciers

and Sjögren-Inlet glaciers). At sector "East" the highest area-loss is found in the earliest observation interval (1985-1990). Davies et al. (2012) also reported higher shrinkage rates for most of the glaciers in this sector in the period 1988-2001 than in the period 2001-2009. Moreover, increased recession is also found in the time period (1995-2005, Fig. 4) at sector "East". This could be indirectly caused by the disintegration of Larsen-A and Prince-Gustav ice shelves. Davies et al. (2012) and

5 Hulbe et al. (2004) proposed that the disintegration of an ice shelf affects the local climate. The air temperatures would rise due to the presence of more ice free water in summers. At Base Marambio, ~100 km east of this sector, about 2°C higher mean annual air temperatures were recorded in the period 1997-2007 as compared to the period 1985-1996 (e.g. Seehaus et al., 2015; Oliva et al., 2017). Unfortunately, no temperature records are available in sector "East" covering this period.

The average changes of flow velocities at each sector also vary strongly (Table 5) in the observation period 1992-2014. On

10 the west coast an increase of 42% is found, whereas in sector "East" the glaciers slowed down by about 69% and at the ice shelf tributaries the ice flow increased on average by 17%. Pritchard and Vaughan (2007) reported an increase in mean flow rate of 7.8% in frame 4923 (the central and northern part of sector "West") and 15.2% in frame 4941 (the southern part of sector "West") for the period 1992-2005. This spatial trend corresponds to our observations, since most of the glaciers with a clear positive velocity trend are located at the southern end of sector "West". However, for the same observation period we

15 discovered a mean increase in flow velocity by 18.9 % in sector "West", which is an about 1.6 times higher acceleration. Pritchard and Vaughan (2007) estimated the mean velocity change by measuring the flow speed at profiles along the flow direction of the glacier, whereas we measured at across glacier profiles at the terminus. If a tidewater glacier speeds-up due to the destabilization of its front, the highest acceleration is found at the terminus (see Seehaus et al., 2015, Fig. 3). Consequently, the different profile locations explain the deviations between both studies.

20 In the following section the observed changes in the individual sectors are discussed in more detail.

5.1 East-Ice-Shelf

In the sector "East-Ice-Shelf" nearly all glaciers showed a rapid and significant acceleration after ice shelf break up and a subsequent slow down (Fig. S14-S26, supplement). A gentle peak in flow speeds is obtained at LAB32 and TPE114 glaciers. They are classified as "stable", since the variations are below the threshold of 0.25 m d^{-1}, according to the categorization in

25 Table 3. Dramatic speed up with subsequent deceleration of former ice shelf tributaries was reported by various authors; e.g. in this sector by Seehaus et al., (2015, 2016) at DBE and Sjögren-Inlet glaciers and further south at Larsen-B embayment by Rott et al. (2011) and Wuite et al. (2015). The velocities reported by Rott et al. (2014) at Sjögren, Pyke, Edgeworth and Drygalski glaciers are generally higher than our findings. The authors measured at locations near the center of the glacier fronts, where the ice flow velocities are typically highest, whereas we measured the median velocities at cross profiles close

30 to the glacier fronts. The different approaches result in different absolute values but equal temporal trends are observed in both studies. Highest peak values of 6.3 m d^{-1} are found at TPE61 Glacier in November 1995 and January 1996. Most

glaciers (Arron Icefall, Drygalski, LAB2, TPE61, TPE62) decelerated towards pre-collapse values and show almost constant flow speeds in recent years, indicating that the glaciers adjusted to the new boundary conditions. At "2558", Boydell, DBE and Sjögren glaciers the deceleration is ongoing and Boydell and DBE glaciers still show increased median flow speeds at the glacier fronts. Thus, these tributary glaciers are still adjusting to the new boundary conditions, as suggested by Seehaus et al. (2015, 2016).

In the 1980s, Prince Gustav Ice Shelf gradually retreated (see Fig. 1) and "2668" Glacier has not been buttressed by the ice shelf since the early 1990s. A deceleration is found in the period 2005-2010 (Fig. S15, supplement). Hence, this glacier may also have experienced a speed up in the early 1990s due to the recession of Prince Gustav Ice Shelf in the 1980s. However, the earliest velocity measurement at "2668" Glacier is only available from February 1996.

The ice shelf in Larsen-Inlet disintegrated in 1987-1988 and earliest velocity measurements are obtained in 1993. Therefore, a potential peak in the flow speed after ice shelf break-up cannot be detected at APPE glaciers (Fig. S16, supplement). The ice flow shows short term variations in the order of 0.2-0.5 m d^{-1} between 1993 and 2014, but no clear long term trend is obvious. Rott et al., (2014) also found nearly constant flow velocities at Pyke Glacier. The authors suggest that the ice flow of APPE glaciers was not strongly disturbed by the ice shelf removal due to the steep glacier surfaces and shallow seabed topography at the glacier fronts (Pudsey et al., 2001).

5.2 East

The glaciers north of the former Prince-Gustav Ice Shelf show a general trend towards lower flow velocities. Eyrie, Russell East, TPE31, TPE32, TPE34, TPE130 and "2731" glaciers experienced a rapid decrease and, except "2731" Glacier, a subsequent stabilization or even gentle acceleration of flow velocities. A significant retreat followed by a stabilization or slight re-advance of the calving front position is also observed at these glaciers. According to Benn and Evans (1998), a small retreat of a glacier with an overdeepening behind its grounding line (i.e. where the bed slopes away from the ice front) can result in a rapid recession into the deepening fjord. The increased calving and retreat of the ice front cause stronger up-glacier driving stress, higher flow speed as well as glacier thinning and steepening (Meier and Post, 1987; Veen, 2002). The glacier front stabilizes when the grounding line reaches shallower bathymetry and ice flow also starts to slowdown. A delay between the front stabilization and slowdown can be caused by thinning and steepening of the glacier. Additionally, the accelerated ice flow can surpass the retreat rates and cause short-term glacier advances in the period of high flow speeds (e.g. Eyrie, Russel East, TPE32 and TPE130 Glacier) (Meier and Post, 1987). This process can be initiated by climatic forcing (Benn and Evans, 1998). Skvarca et al. (1998) reported a significant increase in surface air temperatures at the north-eastern AP in the period 1960-1997 and correlated it with the recession of the Larsen and Prince-Gustav Ice shelves and the observed retreat of tidewater glaciers on James Ross Island in the period 1975-1995 (Skvarca et al., 1995). However, a cooling trend at the AP was revealed by Oliva et al. (2017) and Turner et al. (2016) in the 21st century. Hence, we assume

that the initial recessions of the glaciers in sector "East" were forced by changing climatic conditions before 1992 (the earliest velocity measurements available). Therefore, this initial frontal destabilization and retreat led to high flow speeds at the beginning of our ice dynamics time series and the subsequently observed frontal stabilization caused the deceleration of the ice flow. The fjord geometry significantly affects the dynamics of the terminus of a tidewater glacier (Benn and Evans, 1998; van der Veen, 2002). The tongues of Aitkenhead and "2707" glaciers are split into two branches by nunataks, resulting in rather complex fjord geometries. A retreat from pinning points (e.g. fjord narrowing) causes further rapid recession and higher flow speeds until the ice front reaches a new stable position as observed at Aitkenhead and "2707" Glacier. At TPE10 Glacier a "peaked" flow velocity trend is observed as at Aitkenhead Glacier. No rock outcrop is visible at the terminus, but a potential bedrock bump is identified north of the center of the ice front by visual inspection of optical satellite imagery. Most probably, it acts as a pinning point and prevents further retreat. The front of Broad Valley Glacier is located in a widening fjord. This geometry makes the glacier less vulnerable to frontal changes (Benn and Evans, 1998). Therefore, no significant changes in flow velocities are observed as a consequence of the frontal recession and re-advance.

Diplock and Victory glaciers show a decrease of flow speed during retreat followed by an acceleration combined with frontal advance. This behavior is similar to surge-type glaciers found for example in Alaska – tidewater glacier - (Motyka and Truffer, 2007; Walker and Zenone, 1988) or Karakoram – land terminating - (Rankl et al., 2014). Surge-type glaciers are characterized by episodically rapid down-wasting, resulting in a frontal acceleration and strong advance. At tidewater glaciers the advance can be strongly compensated by increased calving rates in deepwater in front of the glacier. Thus, both glaciers may have experienced a surge cycle in our observation period; however, a longer time series analysis is necessary to prove this hypothesis.

5.3 West

Meredith and King (2005) reported an increase of surface summer temperatures by more than 1°C in the ocean west of the AP since the 1950s. The authors attributed this to atmospheric warming and reduced sea ice production rates. However, Cook et al. (2016) reported cool ocean temperatures along the north-western AP for the period 1945-2009, and an absence of the atmospheric warming at the AP since the turn of the millennium was found by Turner et al. (2016). Thus, the climatic conditions do not show a constant trend. Moreover the glacier geometries differ strongly, and especially in the southern part of the study region, the coastline is dominated by a fractal structure. This factors lead to the heterogeneous pattern of area and flow speed changes in sector "West" as compared to the eastern sectors.

Kunz et al. (2012) observed thinning at the glacier termini along the western AP. An acceleration and terminus retreat can be caused by this process as shown by Benn et al. (2007). However, the authors also point out that changes in ice thickness do not necessarily affect the ice flow and that calving front positions and ice dynamics are strongly dependent on the fjord and glacier geometries.

The large number of glaciers in this sector is analyzed by means of a hierarchical cluster analysis (Section 3.4) and assorted into four groups based on the dissimilarities, resulting in the dendrogram plotted in Fig. 6. Boxplots of the individual input variables of each group are shown in Fig. 7. The correlation between the observed ice dynamics and the glacier geometries of each group are discussed in the following (see also Fig. 7).

Group1 (14 glaciers):

Most glaciers experienced an acceleration. The majority of the glacier basins are "very top-heavy" or "top-heavy" (median $HI = -1.8$), stretching from sea level up to 1892 m on average. The b_{clim} increases toward higher altitudes (van Wessem et al., 2016) and highest values are found in regions between 1000 and 1700 m a.s.l.. Consequently these glaciers receive high mass input in their large high altitude accumulation regions. The accumulation is known to have significantly increased on the AP by 20% since 1850 (Thomas et al., 2008). Pritchard and Vaughan (2007) reported that only a small fraction of the acceleration can be attributed to glacier thickening due to increased mass input. Up-glacier thickening combined with frontal thinning (reported by Kunz et al., 2012) leads to a steepening of the glacier and an increase in driving stress, resulting in faster ice flow (Meier and Post, 1987) as observed in this study. Moreover, a thinning of the terminus reduces the effective basal stress of a tidewater glacier and facilitates faster ice flow (Pritchard and Vaughan, 2007). The flux gate cross sections to catchment size ratios are relatively small, indicating narrowing catchments towards the ice front. The channelized increased ice flow almost compensates for the increased calving rates (due to frontal thinning), resulting in an average shrinkage of the glaciers by only 0.2% in the period 1985-2015. The high flow speeds may outweigh the calving and lead to ice-front advances as measured at Krebs and TPE46 Glacier. The glacier termini of this group are typically located in narrow fjords (Fig. 5) and are clustered in Charcot, Charlotte and Andvord Bay.

Group 2 (19 glaciers)

Glaciers of group 2 are spread all over the study region, with a local clustering in Wilhelmina Bay. Group 2 shows similar h_{max} and FA characteristics to group 1. Area changes are also quite small (-0.1%). Most of the glaciers experienced positive or "peaked" velocities trends. In contrast to group 1 the catchments are in general "bottom-heavy" and some are even "very bottom-heavy". We assume that the constraints are similar to group 1 (increasing b_{clim}, frontal thinning and steepening). However, the additional mass accumulation in the upper regions is smaller due to the "bottom-heavy" glacier geometries. Consequently, the imbalance due to the frontal thinning and up-glacier mass gain is less pronounced as in group 1 and numerous glaciers ("peak" type) started to decelerate after the speed-up, indicating that these glaciers are adjusting to the new boundary conditions.

Group 3 (13 glaciers)

These basins typically show a "bottom-heavy" hypsometry and smaller elevation ranges (in average up to 1103 m a.s.l.). Thus, b_{clim} is relatively low. The smaller mean ice thickness at the termini (161 m, compared to 211 m of all glaciers) of group 3 implies less interaction with the ocean, leading to a small average frontal retreat of ~0.1%. The low frontal ablation does not significantly affect the ice flow, probably due to the flat glacier topography and the low mass input. Consequently, the flow speed is in general stable or even slightly decreases in the observation period. Glaciers of group 3 usually face the open ocean, and do not terminate in narrow fjords (especially in the northern part, Trinity Peninsula).

Group 4 (3 glaciers)

All basins in this group have a "very bottom-heavy" hypsometry and an elevation range comparable to group 3 glaciers. The *FA* factors are in general higher than in group 3, implying that outflow of the catchments is less channelized and the glacier fronts are long compared to the catchment sizes. Therefore, the largest relative area changes, in average -5.1%, are found at glaciers in group 4. However, the absolute frontal retreat is small and does not significantly affect the glacier flow. Note: Group 3 consists of only three samples, limiting the significance.

6 Conclusions

Our analysis expands previous work on ice dynamic changes at the north-western AP in regard to temporal coverage and analysis method. It also spatially extends previous work on changes in ice dynamic to the whole east coast north of 65° S. The spatially and temporally detailed analysis of changes in ice flow speeds and ice front positions revealed different temporal trends in glacier dynamics along the northern AP in the period 1985-2015. The results are in general in line with findings of the previous studies, however along the west coast significantly higher glacier flow was determined and on the eastern side trends in ice dynamics of numerous glaciers were observed for the first time. A large variety of temporal trends in glacier dynamics were observed in our study region and attributed to different forcing and boundary conditions.

On the east side all glacier fronts retreated in the study period, with highest retreat rates observed at former tributaries of the Prince Gustav, Larsen Inlet and Larsen-A ice shelves. Moreover, nearly all the glaciers affected by ice shelf disintegration showed similar temporal trends of ice velocities. The glaciers reacted with a strong acceleration to ice shelf break up followed by a deceleration, indicating that the glaciers adjusted or are still adjusting to the new boundary conditions. Glaciers on the east coast north of the former Prince Gustav Ice Shelf showed in general a significant deceleration and a reduction in frontal ablation. Based on the observed warming trend since the 1960s and the subsequent cooling since 2000 in on the northern AP, we conclude that the initial recession and speed up of the glaciers took place before the start of our observation and that the glaciers are now close to a new equilibrium.

The average flow speed of the glaciers along the west coast of the Antarctic Peninsula significantly increased in the observation period but the total frontal change was negligible. No general pattern is obvious in the ice dynamic changes. However, correlations between the changes in ice dynamics and the glacier geometries of the individual catchments were obtained by applying a hierarchical cluster analysis. Thus, the geometry of the individual glacier basin significantly affects
5 the reaction of the glacier to external forcing.

We conclude that for regions with such a strong spatial variation in topographic and climatic parameters as the AP, it is impossible to derive a regional trend in glacier change by just analyzing single glaciers in this region. Therefore further detailed observation of the current glaciological changes along the AP is needed. Future activities should link remote sensing derived ice dynamics and glacier extent with ocean parameters and ocean models as well as results of regional climate
10 models or ice dynamic models in order to provide a better quantification of mass changes as well as physical processes leading to the observed changes.

Author contributions. T.S. designed the study, processed the SAR data, performed the data analysis and led the writing of the manuscript, in which he received support from all authors. A.C. and A.S. compiled and provided glacier front position data sets. MB initiated the project and coordinated the research.

Competing interests. The authors declare no competing financial interests.

Acknowledgements. This work was supported by the Deutsche Forschungsgemeinschaft (DFG) in the framework of the priority programme "Antarctic Research with comparative investigations in Arctic ice areas" by a grant to M.B. (BR 2105/9-
20 1). MB and TS would like to thank the HGF Alliance "Remote Sensing of Earth System Dynamics" (HA-310) and Marie-Curie-Network International Research Staff Exchange Scheme IMCONet (EU FP7-PEOPLE-2012-IRSES) for additional support. Access to satellite data was kindly provided by various space agencies, e.g. under ESA AO 4032, DLR TerraSAR-X Background Mission Antarctic Peninsula & Ice Shelves, TSX AO LAN0013, TanDEM-X Mission TDX AO XTI_GLAC0264, ASF, GLIMS as well as NASA and USGS.

References

Barrand, N.E., Hindmarsh, R.C.A., Arthern, R.J., Williams, C.R., Mouginot, J., Scheuchl, B., Rignot, E., Ligtenberg, S.R.M., Van Den Broeke, M.R., Edwards, T.L., Cook, A.J., Simonsen, S.B., 2013a. Computing the volume response of the Antarctic Peninsula ice sheet to warming scenarios to 2200. J. Glaciol. 59, 397–409. doi:10.3189/2013JoG12J139

Barrand, N.E., Vaughan, D.G., Steiner, N., Tedesco, M., Kuipers Munneke, P., van den Broeke, M.R., Hosking, J.S., 2013b. Trends in Antarctic Peninsula surface melting conditions from observations and regional climate modeling. J. Geophys. Res. Earth Surf. 118, 315–330. doi:10.1029/2012JF002559

Benn, D.I., Evans, D.J.A., 1998. Glaciers & Glaciation. Arnold.

Benn, D.I., Hulton, N.R.J., Mottram, R.H., 2007. "Calving laws", "sliding laws" and the stability of tidewater glaciers. Ann. Glaciol. 46, 123–130. doi:10.3189/172756407782871161

Berthier, E., Scambos, T.A., Shuman, C.A., 2012. Mass loss of Larsen B tributary glaciers (Antarctic Peninsula) unabated since 2002. Geophys. Res. Lett. 39, L13501. doi:10.1029/2012GL051755Burgess, E.W., Forster, R.R., Larsen, C.F., Braun, M., 2012. Surge dynamics on Bering Glacier, Alaska, in 2008–2011. The Cryosphere 6, 1251–1262. doi:10.5194/tc-6-1251-2012

Cape, M.R., Vernet, M., Skvarca, P., Marinsek, S., Scambos, T., Domack, E., 2015. Foehn winds link climate-driven warming to ice shelf evolution in Antarctica. J. Geophys. Res. Atmospheres 2015JD023465. Doi: 10.1002/2015JD023465

Cook, A. j., Vaughan, D. g., Luckman, A. j., Murray, T., 2014. A new Antarctic Peninsula glacier basin inventory and observed area changes since the 1940s. Antarct. Sci. 26, 614–624. doi:10.1017/S0954102014000200

Cook, A.J., Fox, A.J., Vaughan, D.G., Ferrigno, J.G., 2005. Retreating Glacier Fronts on the Antarctic Peninsula over the Past Half-Century. Science 308, 541–544. doi:10.1126/science.1104235

Cook, A.J., Holland, P.R., Meredith, M.P., Murray, T., Luckman, A., Vaughan, D.G., 2016. Ocean forcing of glacier retreat in the western Antarctic Peninsula. Science 353, 283–286. doi:10.1126/science.aae0017

Cook, A.J., Murray, T., Luckman, A., Vaughan, D.G., Barrand, N.E., 2012. A new 100-m Digital Elevation Model of the Antarctic Peninsula derived from ASTER Global DEM: methods and accuracy assessment. Earth Syst. Sci. Data 4, 129–142. doi:10.5194/essd-4-129-2012

Cook, A.J., Vaughan, D.G., 2010. Overview of areal changes of the ice shelves on the Antarctic Peninsula over the past 50 years. The Cryosphere 4, 77–98. doi:10.5194/tc-4-77-2010

Davies, B.J., Carrivick, J.L., Glasser, N.F., Hambrey, M.J., Smellie, J.L., 2012. Variable glacier response to atmospheric warming, northern Antarctic Peninsula, 1988–2009. The Cryosphere 6, 1031–1048. doi:10.5194/tc-6-1031-2012

De Angelis, H., Skvarca, P., 2003. Glacier Surge After Ice Shelf Collapse. Science 299, 1560–1562. doi:10.1126/science.1077987

Dee, D.P., Uppala, S.M., Simmons, A.J., Berrisford, P., Poli, P., Kobayashi, S., Andrae, U., Balmaseda, M.A., Balsamo, G., Bauer, P., Bechtold, P., Beljaars, A.C.M., van de Berg, L., Bidlot, J., Bormann, N., Delsol, C., Dragani, R., Fuentes, M., Geer, A.J., Haimberger, L., Healy, S.B., Hersbach, H., Hólm, E.V., Isaksen, L., Kållberg, P., Köhler, M., Matricardi, M., McNally, A.P., Monge-Sanz, B.M., Morcrette, J.-J., Park, B.-K., Peubey, C., de Rosnay, P., Tavolato, C., Thépaut, J.-N., Vitart, F., 2011. The ERA-Interim reanalysis: configuration and performance of the data assimilation system. Q. J. R. Meteorol. Soc. 137, 553–597. doi:10.1002/qj.828

Deza, E., Deza, M.M., 2009. Encyclopedia of Distances. Springer Berlin Heidelberg, Berlin, Heidelberg.

Ferrigno, J.G., Cook, A.J., Foley, K.M., Williams, R.S., Swithinbank, C., Fox, A.J., Thomson, J.W., Sievers, J., 2006. Coastal-change and glaciological map of the Trinity Peninsula area and South Shetland Islands, Antarctica, 1843-2001.

Fretwell, P., Pritchard, H.D., Vaughan, D.G., Bamber, J.L., Barrand, N.E., Bell, R., Bianchi, C., Bingham, R.G., Blankenship, D.D., Casassa, G., Catania, G., Callens, D., Conway, H., Cook, A.J., Corr, H.F.J., Damaske, D., Damm, V., Ferraccioli, F., Forsberg, R., Fujita, S., Gim, Y., Gogineni, P., Griggs, J.A., Hindmarsh, R.C.A., Holmlund, P., Holt, J.W., Jacobel, R.W., Jenkins, A., Jokat, W., Jordan, T., King, E.C., Kohler, J., Krabill, W., Riger-Kusk, M., Langley, K.A., Leitchenkov, G., Leuschen, C., Luyendyk, B.P., Matsuoka, K., Mouginot, J., Nitsche, F.O., Nogi, Y., Nost, O.A., Popov, S.V., Rignot, E., Rippin, D.M., Rivera, A., Roberts, J., Ross, N., Siegert, M.J., Smith, A.M., Steinhage, D., Studinger, M., Sun, B., Tinto, B.K., Welch, B.C., Wilson, D., Young, D.A., Xiangbin, C., Zirizzotti, A., 2013. Bedmap2: improved ice bed, surface and thickness datasets for Antarctica. The Cryosphere 7, 375–393. doi:10.5194/tc-7-375-2013

Goodwin, B.P., 2013. Recent Environmental Changes on the Antarctic Peninsula as Recorded in an ice core from the Bruce Plateau. The Ohio State University.

Hulbe, C.L., MacAyeal, D.R., Denton, G.H., Kleman, J., Lowell, T.V., 2004. Catastrophic ice shelf breakup as the source of Heinrich event icebergs. Paleoceanography 19, PA1004. doi:10.1029/2003PA000890

Huss, M., Farinotti, D., 2014. A high-resolution bedrock map for the Antarctic Peninsula. The Cryosphere 8, 1261–1273. doi:10.5194/tc-8-1261-2014

Jiskoot, H., Curran, C.J., Tessler, D.L., Shenton, L.R., 2009. Changes in Clemenceau Icefield and Chaba Group glaciers, Canada, related to hypsometry, tributary detachment, length–slope and area–aspect relations. Ann. Glaciol. 50, 133–143. doi:10.3189/172756410790595796

Kaufman, L., Rousseeuw, P.J., 1990. Finding groups in data: an introduction to cluster analysis, Wiley series in probability and mathematical statistics. Wiley, New York.

Kunz, M., King, M.A., Mills, J.P., Miller, P.E., Fox, A.J., Vaughan, D.G., Marsh, S.H., 2012. Multi-decadal glacier surface lowering in the Antarctic Peninsula. Geophys. Res. Lett. 39, L19502. doi:10.1029/2012GL052823

Lance, G.N., Williams, W.T., 1967. A general theory of classificatory sorting strategies: II. Clustering systems. Comput. J. 10, 271–277. doi:10.1093/comjnl/10.3.271

Marshall, G.J., Orr, A., van Lipzig, N.P.M., King, J.C., 2006. The Impact of a Changing Southern Hemisphere Annular Mode on Antarctic Peninsula Summer Temperatures. J. Clim. 19, 5388–5404. doi:10.1175/JCLI3844.1

McNabb, R.W., Hock, R., O'Neel, S., Rasmussen, L.A., Ahn, Y., Braun, M., Conway, H., Herreid, S., Joughin, I., Pfeffer, W.T., Smith, B.E., Truffer, M., 2012. Using surface velocities to calculate ice thickness and bed topography: a case study at Columbia Glacier, Alaska, USA. J. Glaciol. 58, 1151–1164. doi:10.3189/2012JoG11J249

Meier, M.F., Post, A., 1987. Fast tidewater glaciers. J. Geophys. Res. Solid Earth 92, 9051–9058. doi:10.1029/JB092iB09p09051

Meredith, M.P., King, J.C., 2005. Rapid climate change in the ocean west of the Antarctic Peninsula during the second half of the 20th century. Geophys. Res. Lett. 32, L19604. doi:10.1029/2005GL024042

Motyka, R.J., Truffer, M., 2007. Hubbard Glacier, Alaska: 2002 closure and outburst of Russell Fjord and postflood conditions at Gilbert Point. J. Geophys. Res. Earth Surf. 112, F02004. doi:10.1029/2006JF000475

Oliva, M., Navarro, F., Hrbáček, F., Hernández, A., Nývlt, D., Pereira, P., Ruiz-Fernández, J., Trigo, R., 2017. Recent regional climate cooling on the Antarctic Peninsula and associated impacts on the cryosphere. Sci. Total Environ. 580, 210–223. doi:10.1016/j.scitotenv.2016.12.030

Potocki, M., Mayewski, P.A., Kurbatov, A., Handley, M., Simoes, J.C., Jaña, R., 2011. Detailed Glaciochemical Records from a Northern Antarctic Peninsula Site - Detroit Plateau. AGU Fall Meet. Abstr. 43.

Pritchard, H.D., Vaughan, D.G., 2007. Widespread acceleration of tidewater glaciers on the Antarctic Peninsula. J. Geophys. Res. 112. doi:10.1029/2006JF000597

Pudsey, C.J., Evans, J., Domack, E.W., Morris, P., Valle, R.A.D., 2001. Bathymetry and acoustic facies beneath the former Larsen-A and Prince Gustav ice shelves, north-west Weddell Sea. Antarct. Sci. 13, 312–322. doi:10.1017/S095410200100044X

Rack, W., Rott, H., 2004. Pattern of retreat and disintegration of the Larsen B ice shelf, Antarctic Peninsula. Ann. Glaciol. 39, 505–510.

Rankl, M., Kienholz, C., Braun, M., 2014. Glacier changes in the Karakoram region mapped by multimission satellite imagery. The Cryosphere 8, 977–989. doi:10.5194/tc-8-977-2014

Rau, F., Braun, M., 2002. The regional distribution of the dry-snow zone on the Antarctic Peninsula north of 70°S. Ann. Glaciol. 34, 95–100. doi:10.3189/172756402781817914

Rignot, E., Casassa, G., Gogineni, P., Krabill, W., Rivera, A., Thomas, R., 2004. Accelerated ice discharge from the Antarctic Peninsula following the collapse of Larsen B ice shelf. Geophys. Res. Lett. 31. doi:10.1029/2004GL020697

Rott, H., Floricioiu, D., Wuite, J., Scheiblauer, S., Nagler, T., Kern, M., 2014. Mass changes of outlet glaciers along the Nordensjköld Coast, northern Antarctic Peninsula, based on TanDEM-X satellite measurements. Geophys. Res. Lett. 2014GL061613. doi:10.1002/2014GL061613

Rott, H., Müller, F., Nagler, T., Floricioiu, D., 2011. The imbalance of glaciers after disintegration of Larsen-B ice shelf, Antarctic Peninsula. The Cryosphere 5, 125–134. doi:10.5194/tc-5-125-2011

Scambos, T., Hulbe, C., Fahnestock, M., 2003. Climate-Induced Ice Shelf Disintegration in the Antarctic Peninsula, in: Domack, E., Levente, A., Burnet, A., Bindschadler, R., Convey, P., Kirby, tthew (Eds.), Antarctic Peninsula Climate Variability: Historical and Paleoenvironmental Perspectives. American Geophysical Union, pp. 79–92.

Scambos, T.A., Berthier, E., Haran, T., Shuman, C.A., Cook, A.J., Ligtenberg, S.R.M., Bohlander, J., 2014. Detailed ice loss pattern in the northern Antarctic Peninsula: widespread decline driven by ice front retreats. The Cryosphere 8, 2135–2145. doi:10.5194/tc-8-2135-2014

Scambos, T.A., Bohlander, J., Shuman, C.A., Skvarca, P., 2004. Glacier acceleration and thinning after ice shelf collapse in the Larsen B embayment, Antarctica. Geophys. Res. Lett. 31. doi:10.1029/2004GL020670

Seehaus, T., Marinsek, S., Helm, V., Skvarca, P., Braun, M., 2015. Changes in ice dynamics, elevation and mass discharge of Dinsmoor–Bombardier–Edgeworth glacier system, Antarctic Peninsula. Earth Planet. Sci. Lett. 427, 125–135. doi:10.1016/j.epsl.2015.06.047

Seehaus, T.C., Marinsek, S., Skvarca, P., van Wessem, J.M., Reijmer, C.H., Seco, J.L., Braun, M.H., 2016. Dynamic Response of Sjögren Inlet Glaciers, Antarctic Peninsula, to Ice Shelf Breakup Derived from Multi-Mission Remote Sensing Time Series. Front. Earth Sci. 4. doi:10.3389/feart.2016.00066

Skvarca, P., Rack, W., Rott, H., Donángelo, T.I., 1999. Climatic trend and the retreat and disintegration of ice shelves on the Antarctic Peninsula: an overview. Polar Res. 18, 151–157.

Skvarca, P., Rack, W., Rott, H., Ibarzábal y Donángelo, T., 1998. Evidence of recent climatic warming on the eastern Antarctic Peninsula. Ann. Glaciol. 27, 628–632.

Skvarca, P., Rott, H., Nagler, T., 1995. Satellite imagery, a base line for glacier variation study on James Ross Island, Antarctica. Ann. Glaciol. 21, 291–296.

Strozzi, T., Luckman, A., Murray, T., Wegmuller, U., Werner, C.L., 2002. Glacier motion estimation using SAR offset-tracking procedures. IEEE Trans. Geosci. Remote Sens. 40, 2384–2391. doi:10.1109/TGRS.2002.805079

Thomas, E.R., Marshall, G.J., McConnell, J.R., 2008. A doubling in snow accumulation in the western Antarctic Peninsula since 1850. Geophys. Res. Lett. 35. doi:10.1029/2007GL032529

Turner, J., 2002. Spatial variability of Antarctic Peninsula net surface mass balance. J. Geophys. Res. 107. doi:10.1029/2001JD000755

Turner, J., Colwell, S.R., Marshall, G.J., Lachlan-Cope, T.A., Carleton, A.M., Jones, P.D., Lagun, V., Reid, P.A., Iagovkina, S., 2005. Antarctic climate change during the last 50 years. Int. J. Climatol. 25, 279–294. doi:10.1002/joc.1130

Turner, J., Lu, H., White, I., King, J.C., Phillips, T., Hosking, J.S., Bracegirdle, T.J., Marshall, G.J., Mulvaney, R., Deb, P., 2016. Absence of 21st century warming on Antarctic Peninsula consistent with natural variability. Nature 535, 411–415. doi:10.1038/nature18645

van Lipzig, N.P.M., King, J.C., Lachlan-Cope, T.A., van den Broeke, M.R., 2004. Precipitation, sublimation, and snow drift in the Antarctic Peninsula region from a regional atmospheric model. J. Geophys. Res. Atmospheres 109, D24106. doi:10.1029/2004JD004701

van Lipzig, N.P.M., Meijgaard, E. van, Oerlemans, J., 2002. The spatial and temporal variability of the surface mass balance in Antarctica: results from a regional atmospheric climate model. Int. J. Climatol. 22, 1197–1217. doi:10.1002/joc.798

van Wessem, J.M., Ligtenberg, S.R.M., Reijmer, C.H., van de Berg, W.J., van den Broeke, M.R., Barrand, N.E., Thomas, E.R., Turner, J., Wuite, J., Scambos, T.A., van Meijgaard, E., 2016. The modelled surface mass balance of the Antarctic Peninsula at 5.5 km horizontal resolution. The Cryosphere 10, 271–285. doi:10.5194/tc-10-271-2016

van der Veen, C.J., 2002. Calving glaciers. Prog. Phys. Geogr. 26, 96–122. doi:10.1191/0309133302pp327ra

Walker, K.-M., Zenone, C., 1988. Multitemporal Landsat multispectral scanner and thematic mapper data of the Hubbard Glacier region, southeast Alaska. Photogramm. Eng. Remote Sens. 54, 373–376.

Ward, J.H., 1963. Hierarchical Grouping to Optimize an Objective Function. J. Am. Stat. Assoc. 58, 236–244. doi:10.1080/01621459.1963.10500845

Wendt, J., Rivera, A., Wendt, A., Bown, F., Zamora, R., Casassa, G., Bravo, C., 2010. Recent ice-surface-elevation changes of Fleming Glacier in response to the removal of the Wordie Ice Shelf, Antarctic Peninsula. Ann. Glaciol. 51, 97–102.

Wuite, J., Rott, H., Hetzenecker, M., Floricioiu, D., De Rydt, J., Gudmundsson, G.H., Nagler, T., Kern, M., 2015. Evolution of surface velocities and ice discharge of Larsen B outlet glaciers from 1995 to 2013. The Cryosphere 9, 957–969. doi:10.5194/tc-9-957-2015

Figures
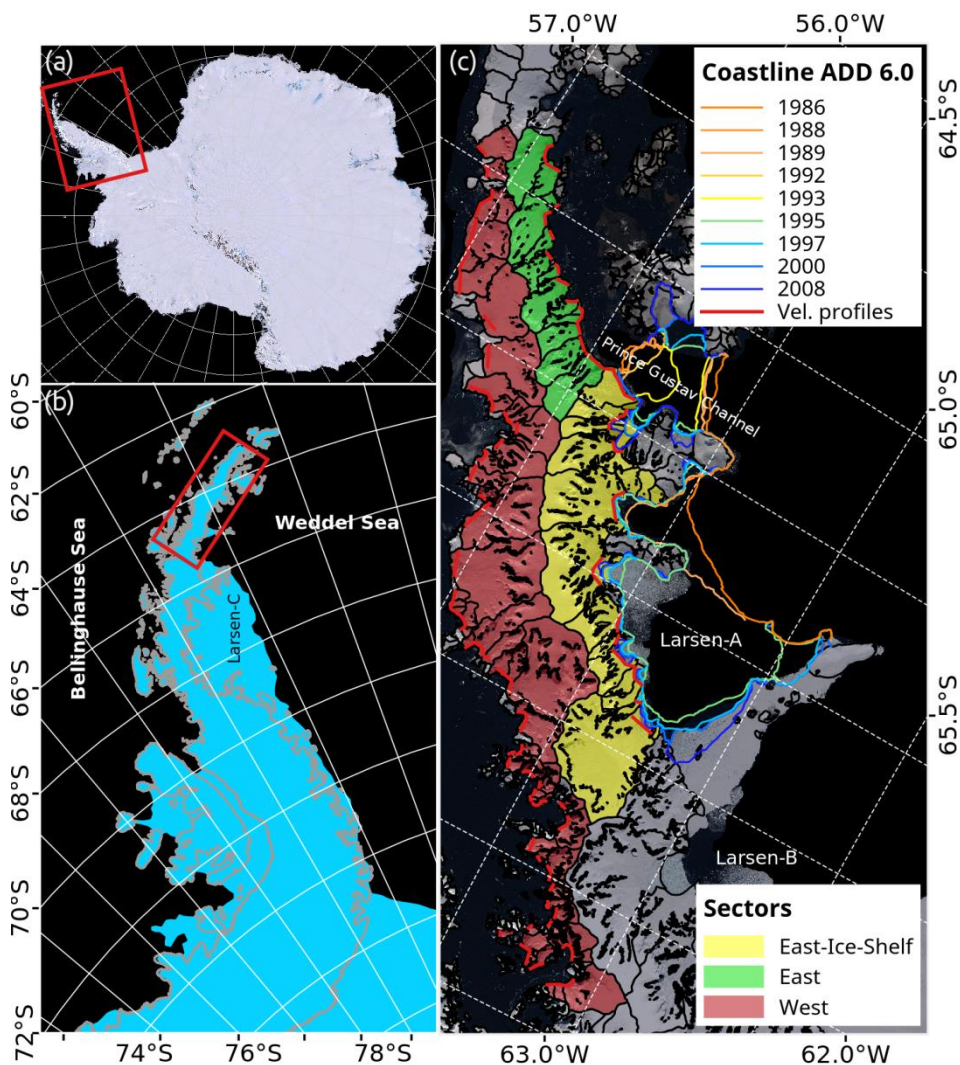
5   **Figure 1.** Panels **(a)** and **(b)**. Location of study site on the Antarctic Peninsula. Panel **(c)**. Separation of study site in 3 sectors and retreat states of Prince-Gustav and Larsen-A ice shelves. Red lines: profiles at glacier front for velocity measurements. Map base, Landsat LIMA Mosaic © USGS, coastlines and catchment delineations from SCAR Antarctic Digital Database 6.0.
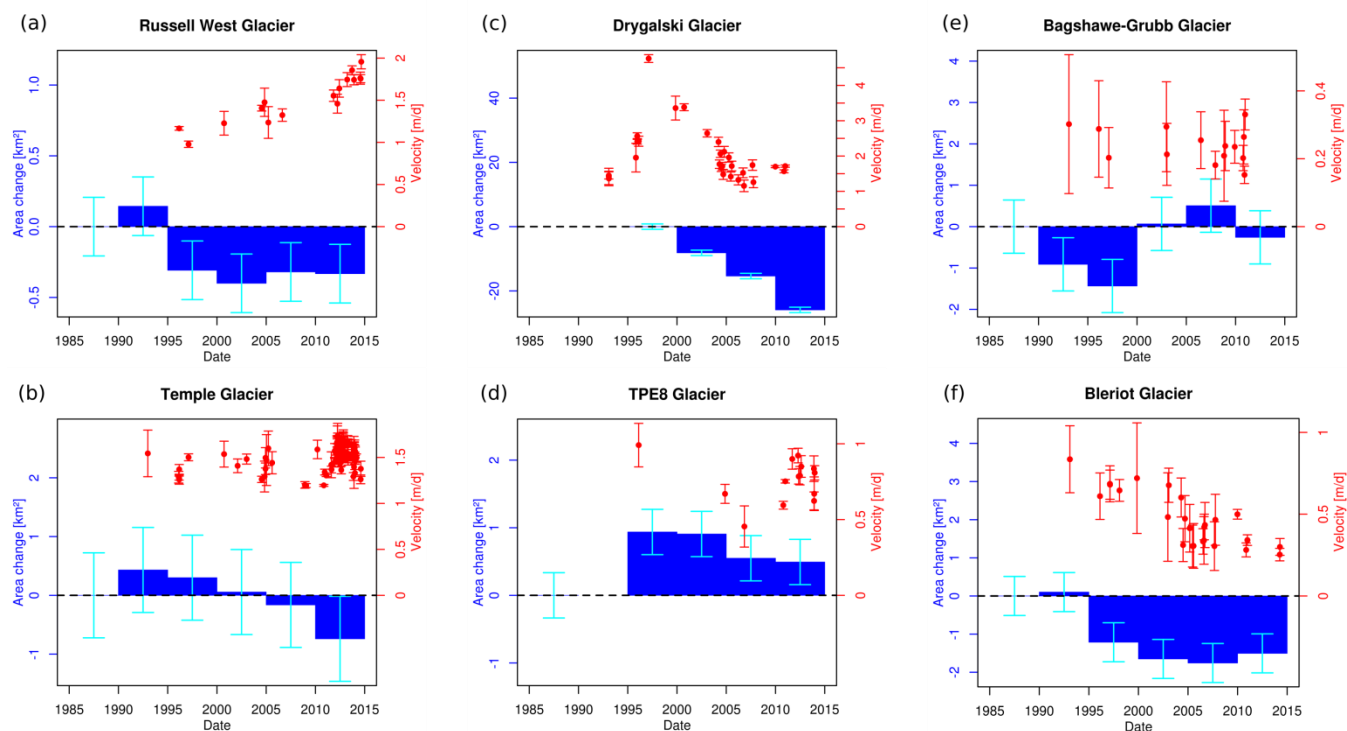
Figure 2. Temporal trend of surface velocity (red) and area (blue) changes of selected glaciers in the study region.
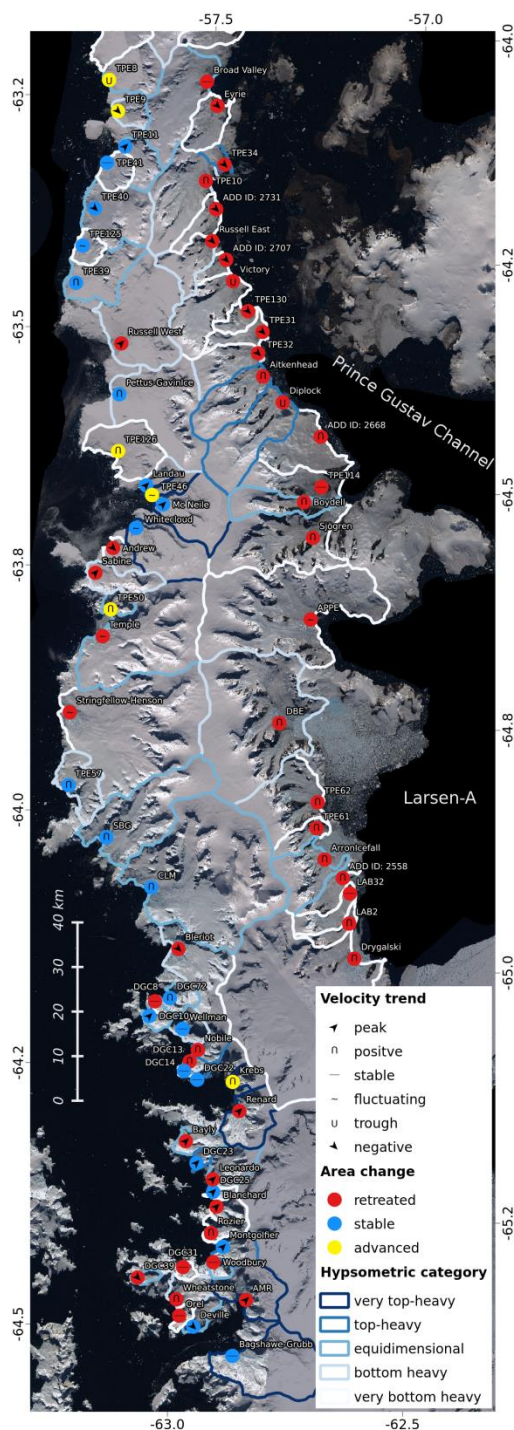
Figure 3. Categorizations of glaciers to temporal trends in area changes (dots) and flow velocities (symbols). Colors of catchment delineation indicate Hypsometric categories according to Jiskoot et al. (2009). Background: Landsat LIMA Mosaic © USGS
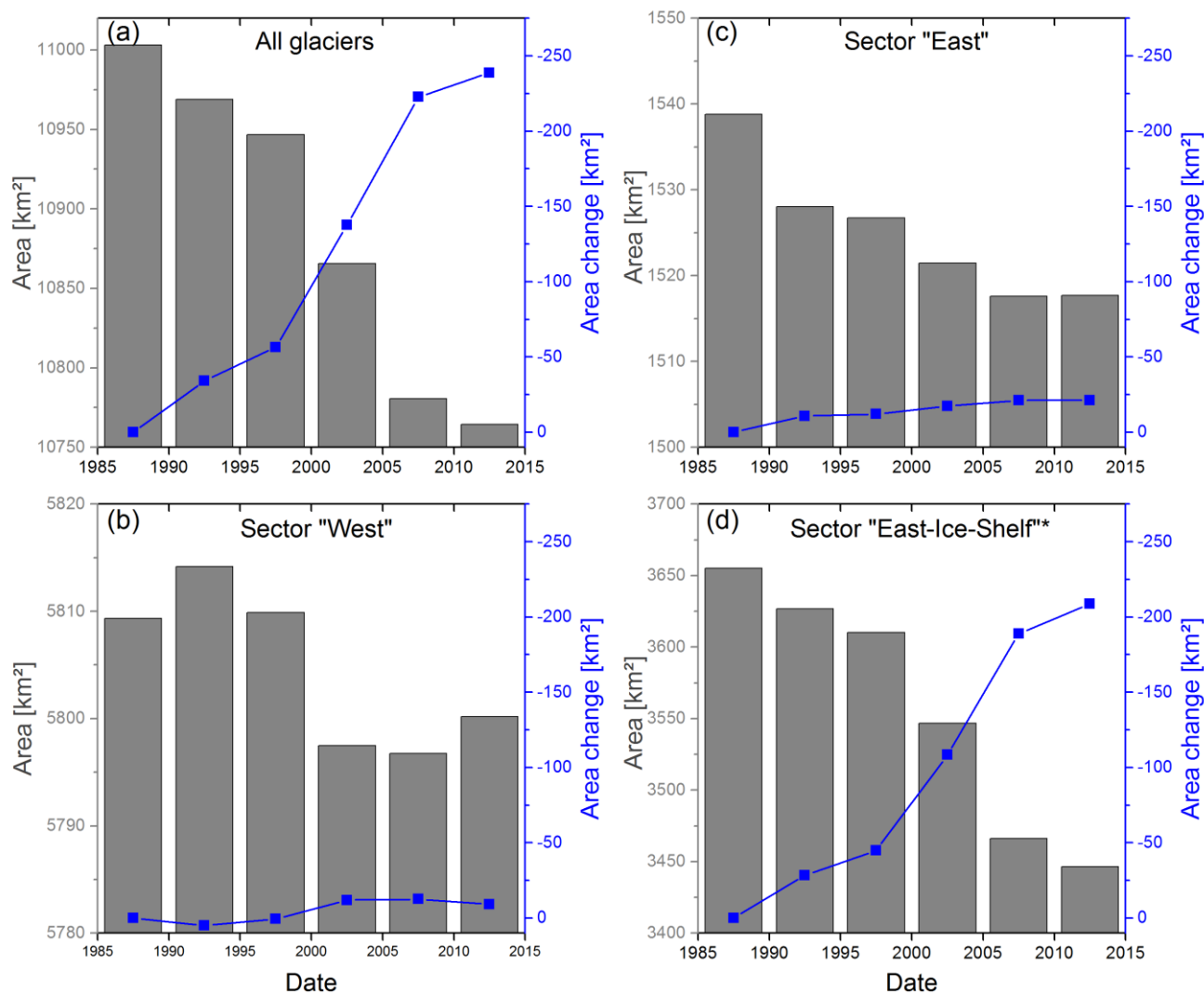
Figure 4. Total glacier area (gray bars) of the whole study site (Panel **(a)**) and of the individual sectors (Panels **(b)**-**(d)**) in the period 1985-2015. Changes in glacier area (blue points) are relative to the measurements in time interval 1985-1990. Note the different scaling of the y-axes. In sector "East", area changes before 1995 are only measured at Larsen-Inlet tributaries (APPE glaciers).
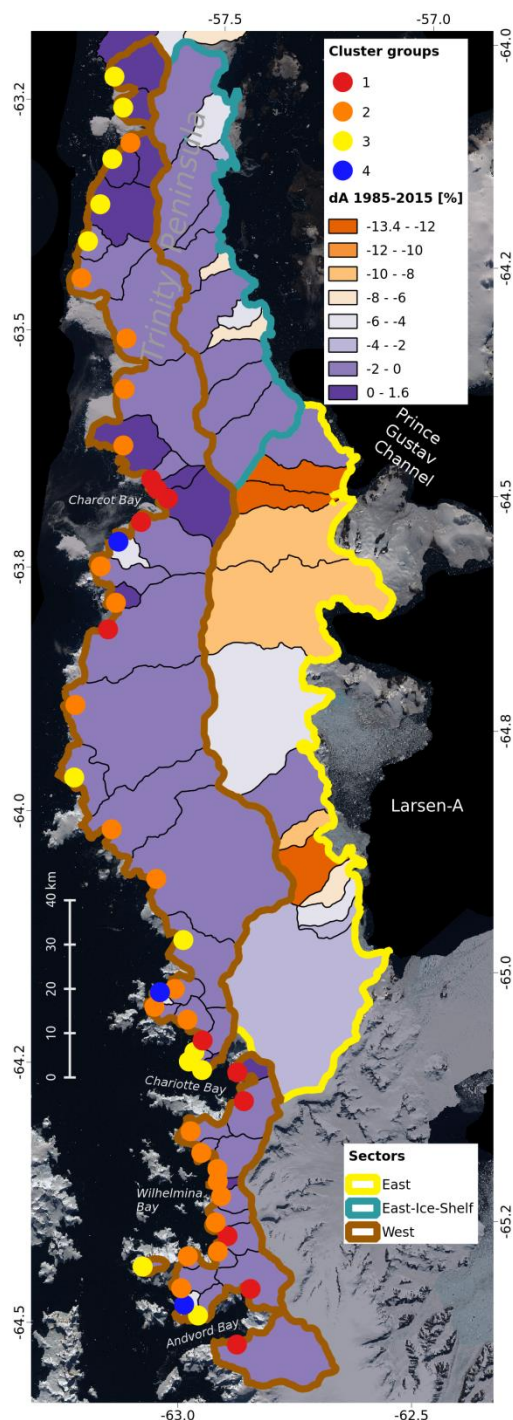
Figure 5. Spatial distribution of glacier types along the west coast. Glaciers are group based on a hierarchical cluster analysis (dots). In Section 5.3 the characteristics of the groups are discussed in detail. Catchment colors: relative area change in the period 1985-2015. Colored polygons: Boundaries of the three regional sectors.
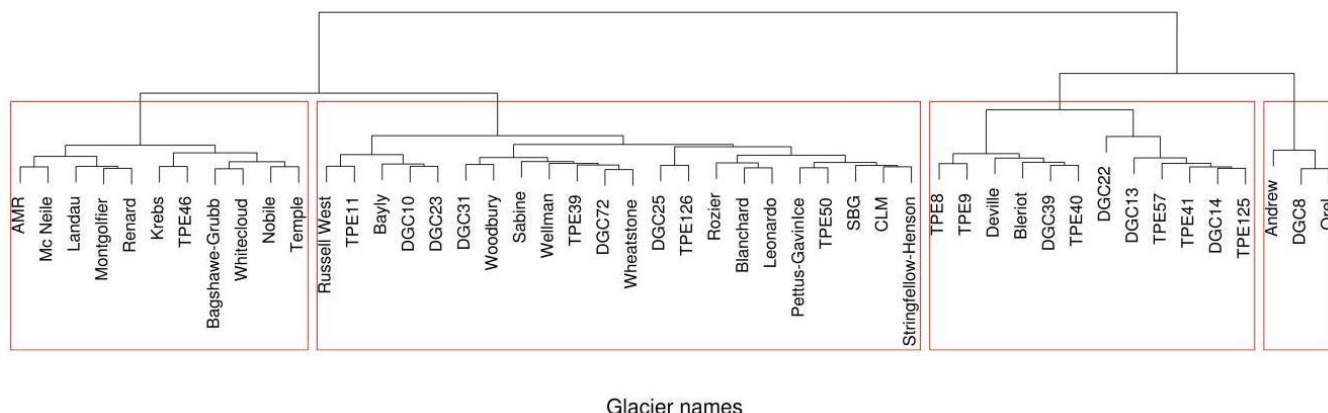
Figure 6. Dendrogram of hierarchical cluster analysis of glaciers in sector "West". The glaciers are assorted in four groups (red rectangles). In Section 5.3 the characteristics of the groups are discussed in detail.
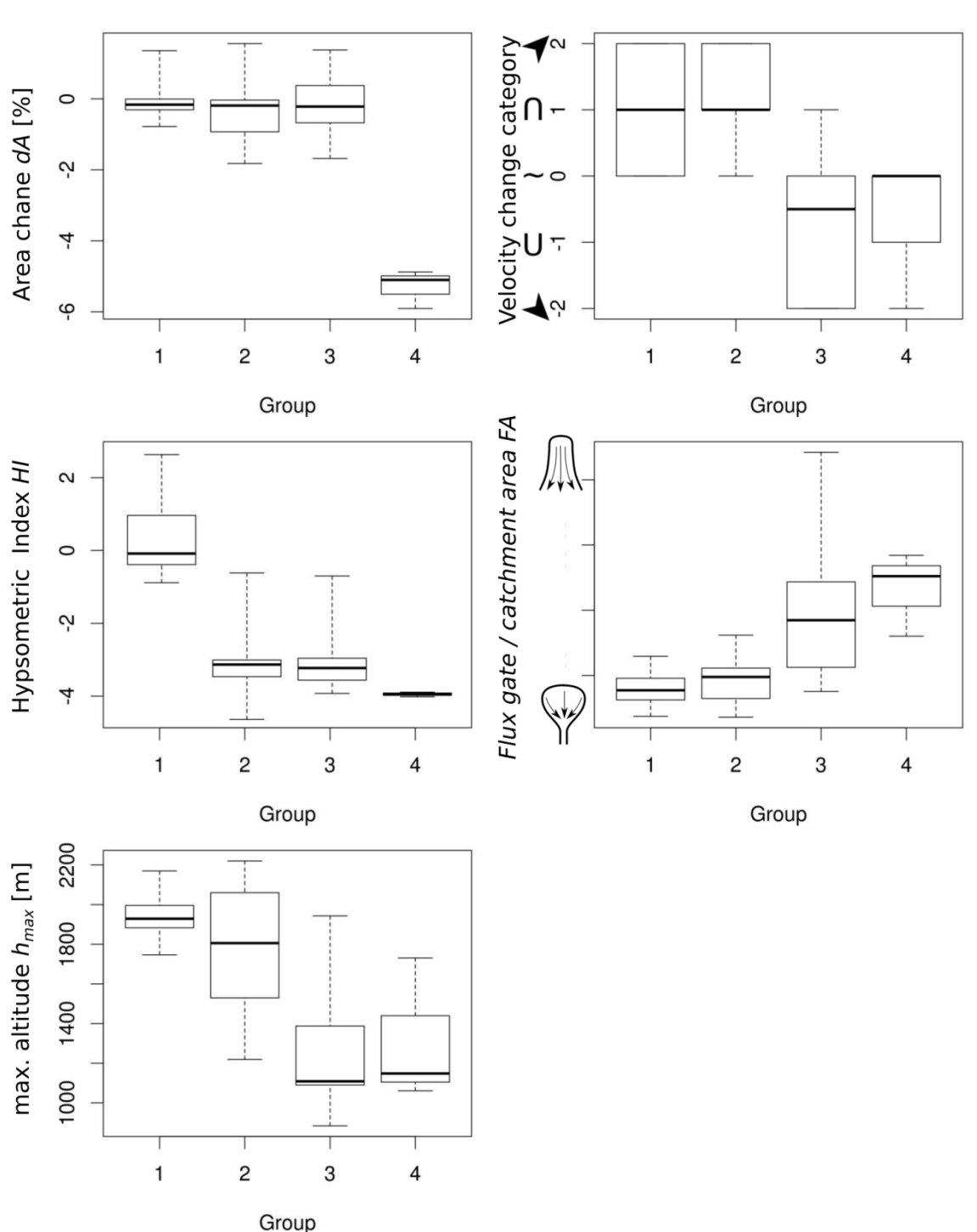
Figure 7. Boxplots of cluster analysis input variables (Sector "West") for each group. Whiskers extend to the most extreme data points.

Tables

Table 1. Used abbreviations of glacier names

Abbreviation	Glacier names
AMR	Arago-Moser-Rudolph
APPE	Albone-Pyke-Polaris-Eliason
CLM	Cayley-Lilienthal-Mouillard
DBE	Dinsmoor-Bombardier-Edgeworth
SBG	Sikorsky-Breguet-Gregory

Table 2. Overview of SAR sensors and specifications used in this study. Intensity tracking parameters are provided in pixels [p] in slant range geometry.

Platform	Sensor	Mode	SAR band	Repetition cycle [d]	Time interval	Tracking patch sizes [p x p]	Tracking step size [p x p]
ERS-1/2	SAR	IM	C band	35/1	08. December 1992	48x240	5x25
					02. April 2010	64x320	
RADARSAT 1	SAR	ST	C band	24	10. September 2000	48x192	5x20
					03. September 2006	64x256	
						64x256	
Envisat	ASAR	IM	C band	35	05. December 2003	32x160	5x25
					16. August 2009	64x320	
						128x640	
ALOS	PALSAR	FBS	L band	46	18. May 2006	64x192	10x30
					17. March 2011	96x192	
						128x384	
TerraSAR-X TanDEM-X	SAR	SM	X band	11	14. October 2008	128x128	25x25
					22. December 2014	256x256	
						512x512	

Table 3. Description of velocity change categories. *Ratings used for cluster analysis

Category	Description	Rating*
positive	Long term increase of flow speed	2
peak	Increase of flow speed with subsequent deceleration	1
stable	Variability of measurements < 0.25 m d^{-1}	0
fluctuating	Short term speed-ups and deceleration, no clear trend	0
trough	Decrease of flow speed with subsequent acceleration	-1
negative	Long term decrease of flow speed	-2

Table 4. Hypsometric categories based on the Hypsometric Index according to Jiskoot et al., (2009)

Hypsometric Index (HI)	Hypsometric categories
$HI < -1.5$	Very top-heavy
$-1.5 < HI < -1.2$	Top-heavy
$-1.2 < HI < 1.2$	Equidimensional
$1.2 < HI < 1.5$	Bottom-heavy
$HI > 1.5$	Very bottom-heavy

Table 5. Summary of observed parameters for each sector and all glaciers. l_f – length of ice front; A – Glacier area in the respective period; dA – Change in glacier area between 1985 and 2015; dt: mean time period of velocity measurements, v_s – mean of earliest velocity measurements (1992-1996); v_E – mean of latest velocity measurements (2010-2014), dv – mean velocity change; n_v – sum of velocity measurements in the observation period (dt)

Sector	East	East-Ice-Shelf	West	All glaciers
l_f [m]	85114	127909	268763	481786
$A_{1985\text{-}1990}$ [km²]	1538.78	3655.13	5809.33	11003.23
$A_{2010\text{-}2015}$ [km²]	1517.71	3446.54	5800.18	10764.42
dA [km²]	-21.07	-208.59	-9.14	-238.81
dt [a]	18.79	19.05	20	19
v_S [m d^{-1}]	0.995	0.480	0.427	0.537
v_E [m d^{-1}]	0.307	0.561	0.605	0.545
dv [m d^{-1}]	-0.688	0.081	0.177	0.008
n_v	319	584	1600	2503